Sidewall passivation assisted by a silicon coverplate during Cl_2-H_2 and HBr inductively coupled plasma etching of InP for photonic devices

S. Bouchoule,[a] G. Patriarche, S. Guilet, L. Gatilova,[b] and L. Largeau
Laboratoire de Photonique et de Nanostructures (LPN)—CNRS, Route de Nozay, 91460 Marcoussis, France

P. Chabert
Laboratoire de Physique et Technologie des Plasmas (LPTP)—CNRS—Ecole Polytechnique, Route de Saclay, 91128 Palaiseau, France

(Received 26 November 2007; accepted 25 February 2008; published 1 April 2008)

Energy dispersive x-ray (EDX) spectroscopy coupled to transmission electron microscopy (TEM) is used to analyze the passivation layer deposited on the sidewall of InP submicron patterns etched in Cl_2-H_2 and HBr inductively coupled plasmas. It is shown that a thin Si-containing layer is deposited on the sidewalls of the etched patterns, resulting from the reaction of Cl_2 or HBr with the Si wafer used as the sample tray. For Cl_2-containing plasma, the deposition layer becomes thicker when hydrogen is added to the gas mixture, leading to highly anisotropic InP etching at an optimized H_2 percentage. A similar effect is obtained in HBr plasma by increasing the ICP power. When O_2 is added to the gas mixture, the deposited layer is changed from Si rich to more stoichiometric silicon oxide (SiO_2) and the passivation effect is enhanced. EDX-TEM analysis has also been carried out on InP samples etched in Cl_2-N_2 plasma for comparison. A similar impact of the coverplate material on the sidewall profile is evidenced, the InP sidewall being moreover strongly In deficient in this case. These results give useful guidelines to define anisotropic etching processes scalable to large-diameter InP wafers. © *2008 American Vacuum Society.*
[DOI: 10.1116/1.2898455]

I. INTRODUCTION

High-aspect-ratio etching of InP-based heterostructures is a critical building block for photonic device fabrication. A dry-etching process that can produce highly anisotropic profiles and smooth sidewalls free from undercuts or notches is indeed required to minimize the optical scattering losses in key elements such as deeply etched facets and mirrors, deep ridge waveguides, ring resonators, or micropillar cavities. Inductively coupled plasma (ICP) etching of InP has been widely developed for this purpose in the past years using Cl_2 as the main etching gas, with few studies also devoted to HBr. Pure Cl_2 or HBr atmospheres generally leading to significant undercuts,[1–3] additive gas have been added to achieve anisotropic etching of high-aspect-ratio patterns. N_2 is known as a strongly passivating gas due to nitridation of the InP surface,[4,5] and anisotropic etching has been reported for $HBr-N_2$ (Ref. 3) and Cl_2-N_2 (Refs. 6 and 7) gas mixtures. Cl_2-H_2 (Ref. 2) or Cl_2-H_2-Ar (Ref. 1) gas mixtures have also been developed to obtain smooth and vertical profiles adapted to the definition of deep ridge waveguides and ring resonators. Several mechanisms have been suggested to date in order to account for the onset of the anisotropic regime. Anisotropic etching of InP/InGaAsP heterostructures in Cl_2-H_2-Ar chemistry may result from a balancing effect between the Cl_2-H_2 chemical etch and the Ar physical component, with all the epitaxial layers being etched at approximately the same rate.[1] Hydrogen passivation of the InP surface has also been mentioned in order to explain the reduced lateral etching.[8] However, a detailed investigation of the passivation mechanisms controlling the etching anisotropy has not been carried out. In a previous work on Cl_2-H_2 chemistry, we highlighted that the H_2 concentration was an important parameter to control the anisotropy and we also evidenced that using a Si wafer as sample tray was essential to obtain smooth and vertical sidewalls.[2] Still using a Si tray, we recently demonstrated vertical and smooth HBr etching of ridge laser waveguides.[9] In this article, we employ *ex situ* energy dispersive x-ray spectroscopy coupled to transmission electron microscopy (EDX-TEM) to investigate the sidewall passivation of InP etched in Cl_2-H_2 and HBr atmospheres when a Si wafer acts as the electrode coverplate. This configuration corresponds to most commercial ICP etch systems having an electrode diameter of 4 in. or more, and used to etch InP samples with typical dimensions of 2 in. or less. We show that anisotropic etching is obtained thanks to the deposition on the InP sidewalls of a Si-containing layer that becomes thicker when hydrogen is added to chlorine. A similar passivation effect is observed in HBr chemistry, the passivation layer consisting mainly of SiO(Br) instead of SiO(Cl). When O_2 is intentionally added to the gas mixture, the deposited layer is changed from Si rich to more stoichiometric silicon oxide (SiO_2). Finally, *ex situ* EDX-TEM analysis has also been carried out on InP samples etched in Cl_2-N_2 plasma for comparison. A similar impact of the coverplate material is observed with this chemistry. A thick SiOP amorphous layer is formed on the InP sidewalls, the sidewall being significantly In deficient.

[a]Electronic mail: sophie.bouchoule@lpn.cnrs.fr
[b]Also at Laboratoire de Physique et Technologie des Plasmas, CNRS—Ecole Polytechnique, Palaiseau, France.

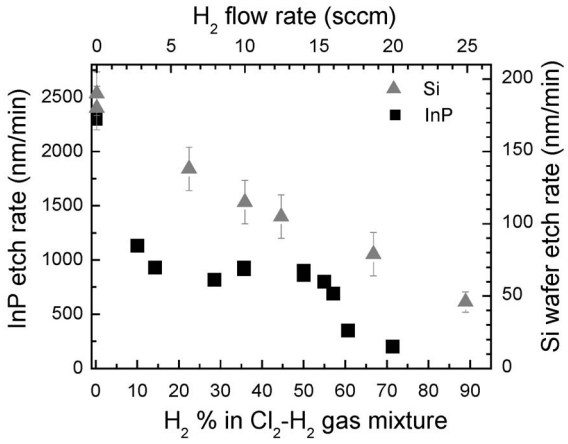

FIG. 1. InP etch rate (squares, left vertical axis), and Si-wafer etch rate (triangles, right vertical axis), as a function of H_2 percentage in the Cl_2–H_2 mixture. The other eching parameters are 800 W ICP power, 0.5 mT, −140 V dc bias, and 28 SCCM total flow rate. The electrode temperature is fixed to 150 °C, the InP samples are nonthermalized.

II. GENERAL EXPERIMENTAL CONDITIONS

The samples were etched in a Sentech SI-500 planar triple spiral antenna ICP etch system described elsewhere.[2] The reactor chamber is made of aluminum. The ICP source is coupled to the plasma through an Al_2O_3 ceramic window. The sample is deposited on a 4 in. tray transferred to the reactor chamber via a load lock, and mechanically clamped above the rf-biased electrode with an Al_2O_3 ceramic clamping ring. The tray (also named electrode coverplate) is thermally coupled to the electrode with He backside cooling. In the following experiments, no heat-conducting grease was used to attach the samples to the tray (nonthermalized samples).

The samples used for the study were bulk *n*-doped InP(100) substrates. The wafers were patterned with a hybrid metal-dielectric mask consisting of 50 nm Cr deposited on a 550 nm thick SiN_x layer using the lift-off technique, with subsequent etching of SiN_x by SF_6/CHF_3 reactive ion etching using Cr as a mask. The wafers were then cut into 7 $\times$7 mm^2 samples for the study. The patterns were defined by electron beam lithography and consisted of 1 μm wide ridges, and of arrays of micropillars with a diameter varying from 0.7 to 0.1 μm by step of 0.1 μm. The etch depth was fixed to 3 μm for all the etching experiments. The smallest diameter still available after 3 μm deep etching depended on the process anisotropy, but sub-0.7-μm diameter pillars suitable for TEM inspection were generally observed by scanning electron microscopy (SEM) in all cases. The maximum aspect ratio was estimated from SEM inspection by identifying the pillar of smallest diameter that could be etched to an etch depth of 3 μm.

Ex situ EDX-TEM analysis of the micropillar sidewalls was then carried out with the following procedure: the etched micropillars were cut from the substrate and dispersed on a carbon membrane for TEM inspection of the pillars sidewalls. The presence of any passivation layer different from InP could be detected with a spatial resolution better than 1 nm. The composition of this layer could be analyzed with an estimated spatial resolution of ~5 nm, using the EDX spectroscopy system installed in the microscope with the transmitted electron beam as the excitation source. When a passivation layer was present on the sidewalls, but when its thickness was smaller or comparable to the EDX analysis resolution, the precise quantification of its composition became difficult. Nevertheless, the layer composition has been roughly estimated in this case by assuming that the amorphous layer did not contain any In and P elements, and by ignoring the In and P peaks when calculating the atomic percentage of the constituting elements from the EDX spectra.

After etching and before EDX-TEM *ex situ* analysis, the samples were immersed in isopropanol in order to limit the reaction of the passivation layer with ambient air. The dielectric mask was not removed.

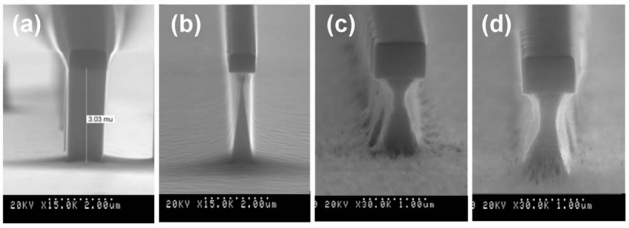

FIG. 2. SEM images of the ridge mesas etched for t=220 s with 800 W ICP power, −140 V dc bias, 0.5 mT, and Cl_2/H_2=18/10 SCCM using different 4 in. diameter sample trays: (a) *c*-Si wafer, (b) aluminum, (c) quartz, and (d) alumina. The electrode temperature is fixed to 150 °C, InP samples are nonthermalized.

III. Cl_2–H_2 CHEMISTRY

The etching parameter values corresponded to those previously optimized for the etching of InP-based ridge waveguides,[2] e.g., pressure of 0.5 mTorr, ICP power of 800 W, dc bias voltage of −140 V, and total gas flow of 28 SCCM (SCCM denotes cubic centimeter per minute at STP). The InP etch rate is reported in Fig. 1 as a function of H_2 percentage in the gas mixture. The etch rate of the 4 in. Si tray was measured simultaneously by patterning the Si wafers with a SiO_2 mask forming 20 μm wide ridge mesa spaced by 500 μm in the center area of the wafer. In pure Cl_2, a high InP etch rate of more than 2 μm/min was achieved but a significant undercut was observed, and we previously showed that smooth and anisotropic etching could be obtained by increasing the H_2 % in the 35%–45% range.[2] This anisotropic regime also coincides with the local maximum in the InP etch rate curve as seen in Fig. 1, which corresponds to a maximum in H concentration in the plasma as deduced from actinometry measurements.[10] The strong influence of the coverplate material on the etching results is illustrated in Figs. 2(a)–2(d), showing the SEM images of the ridge profiles obtained for the same etching conditions with Cl_2/H_2=18/10 SCCM (H_2 %=35.7%) successively reproduced with *c*-Si, Al, SiO_2 (quartz), and Al_2O_3 (alumina

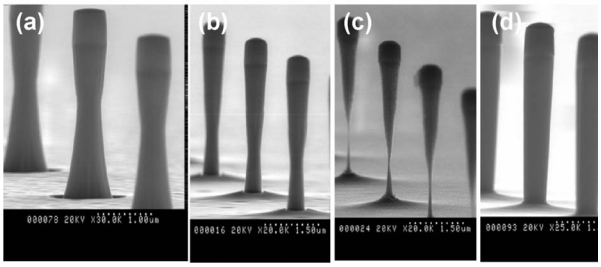

FIG. 3. SEM images of the 0.6-μm diameter micropillars etched with Cl_2-Ar chemistry with Ar% = 0% (a), Ar% = 39% (b), and Ar% = 70% (c). The SEM image of a micropillar of same diameter etched with Cl_2/H_2 (H_2% = 35.7%) is shown for comparison (d). A *c*-Si wafer is used as the sample tray.

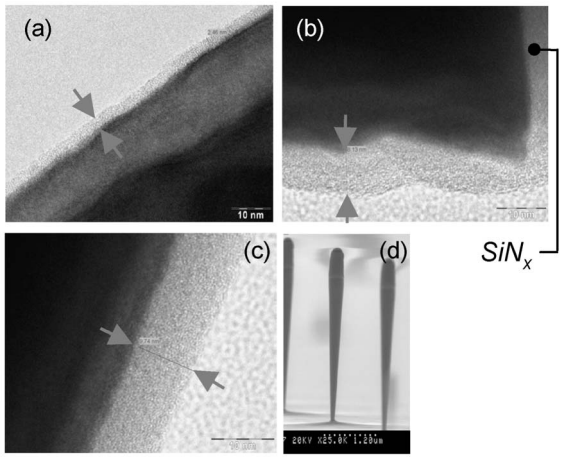

FIG. 4. Typical TEM images of the micropillar sidewalls for the (a) Cl_2, (b) Cl_2-Ar, and (c) Cl_2-H_2 chemistries. (d) SEM image of the pillar of smallest diameter (0.3 μm, aspect ratio > 10) safely etched with the Cl_2-H_2 chemistry.

99.7%) coverplates. It can first obviously be deduced from the SEM images that the reaction products of silicon significantly contribute to the smooth etching of the InP surface. This is consistent with similar observations already reported for InP and GaN ICP etching with Cl_2 chemistry.[11,12] More interestingly, the process anisotropy is only obtained with the Si tray, indicating that the sidewall passivation mechanism depends on silicon.

In order to investigate in more details by EDX-TEM analysis the passivation mechanism when a Si tray is used, a series of three samples were etched using Cl_2 plasma, Cl_2-H_2 plasma with H_2 % = 35.7%, and Cl_2-Ar plasma. For Cl_2-Ar plasma, a set of experiments was preliminary conducted to define the Ar percentage leading to the less undercut profile, with all etching parameters kept similar to the Cl_2-H_2 case except for H_2 being replaced by Ar. It was observed that the InP etch rate continuously decreases when increasing the Ar percentage (from more than 2 μm/min for pure Cl_2 to 0.42 μm/min for Ar % = 80%), but that a smooth anisotropic profile could never be obtained, as illustrated in Fig. 3 showing the SEM images of 0.6-μm diameter micropillars etched with Ar % = 0%, 39%, and 70%. The sample etched with an Ar percentage of 39%, close to the H_2 percentage in the Cl_2-H_2 anisotropic process, was chosen for the EDX-TEM analysis. TEM images of the pillar sidewalls are reported in Figs. 4(a)–4(c) for the three cases. An amorphous layer is observed on the sidewalls, which thickness generally gradually decreases from the top part of the pillar to the bottom of the pillar. In the Cl_2 case, the layer is very thin: the measured thickness is of 2 to 3 nm, and is almost constant from the top to the bottom of the pillar. For the Cl_2-Ar case, the average thickness of the amorphous layer is of 10 nm on the top of the pillar, and is reduced to 2–3 nm on the bottom part. For the Cl_2-H_2 case, the average amorphous layer thickness is of 15 nm on top of the pillar, and continuously decreases down to 2–3 nm on the very bottom of the pillar. It should be noted that this layer is also present on the dielectric mask sidewall, as can be seen in Fig. 4(b). TEM inspection also evidenced that the smoothest sidewalls are obtained with the Cl_2-H_2 chemistry. Beneath the amorphous layer, the material is crystalline and EDX analysis showed that it is InP. The composition (atomic percentage) of the amorphous layer deduced from the EDX spectra is given in Table I for the three samples. The InP etch rate, the Si wafer etch rate, the equivalent Si flux calculated from the Si etch rate assuming a Si density of 5×10^{22} at./cm^3, and the amorphous layer thickness are also reported in the table. The amorphous layer is composed of silicon in the three cases. For Cl_2 chemistry, the very thin layer is estimated to be SiO_2. The deposition rate of this amorphous layer on the InP sidewall is apparently too low or its etch rate by the chlorine atoms is too high to prevent lateral etching of InP and undercut. In the Cl_2-Ar case, the amorphous layer also consists of SiO_2. Although this layer is thicker on the top part of the pillar than in the pure Cl_2 case, the deposition rate is apparently still too low to allow for smooth anisotropic etching. In the case of the Cl_2-H_2 chemistry leading to the thickest passivation layer, the layer appears to be more Si rich than in the two other cases, the Si/O ratio being around 1. It should be noted that possible H incorporation in the layer cannot be detected by EDX analysis. The thicker and apparently more Si-rich layer is obtained despite the fact that the Si wafer etch rate is the lowest, as can be deduced from Table I. From these observations, we first conclude that the deposition of a Si-containing amorphous layer is the origin of the anistropic etching of InP, and second, we suggest that the deposition of the Si-rich amorphous layer deposition is enhanced by H addition in the plasma. Finally, the results of the *ex situ* analysis reported in Table I show that a large amount of oxygen is also incorporated in the passivation layer. The possible origin and role of oxygen will be discussed in Sec. V.

IV. HBr CHEMISTRY

HBr being a Si etchant and HBr plasma containing H, it can be expected from the above results that anisotropic etching of InP may also be obtained in HBr plasma, despite earlier reports showing that pure HBr etching leads to undercut profiles.[3,13] Indeed, we recently demonstrated HBr ICP

TABLE I. InP etch rate, 4 in. Si wafer etch rate (and Si equivalent flux, Φ_{Si}), average thickness of the passivation layer measured on the top part of the pillar, and average passivation layer composition in atomic percentage, for the Cl_2, Cl_2-Ar, Cl_2-H_2, and HBr process. In the Cl_2 case, the thickness of the passivation layer is smaller than the spatial resolution of the EDX analysis.

Process	Etch rate (nm/min)		Passivation layer							
				Average composition (at %)						
Gas flow rate (SCCM)	InP	Si [Φ_{Si} (SCCM)]	Thickness (nm)	Si	O	Br	Cl	P	In	Al
Cl_2 (28)	2400	220 (2.8)	2–3	35	65	···	···	···	···	···
Cl_2(17)/Ar(11)	1380	165 (2.1)	8–10	38	62	···	···	···	···	···
Cl_2(18)/H_2(10)	850	140 (1.8)	10–15	49	49	···	2	···	···	···
HBr (10), 1100 W ICP	570	95 (1.2)	70	66	22	5	···	7	···	···

smooth etching of InP ridge waveguides with highly vertical profile under optimized ICP power and pressure conditions.[9]

Figure 5 shows the typical evolution of the InP etch rate in HBr chemistry when the ICP power is increased. A Si wafer was used as the sample tray, and the other etching parameters were −140 V dc bias, 1 mT, and 10 SCCM flow rate. A similar etch rate behavior was obtained in the 0.35–1 mT pressure range. The Si wafer etch rate is also reported in the figure. Below a typical ICP power value of 200 W, the InP etch rate is low and the etched surface of the samples was rough, indicating that the flux of ions impinging the surface was not sufficient to elevate the sample at the necessary temperature. This is consistent with positive ion current density measurements previously performed in the same plasma conditions with a rf planar probe installed on the reactor walls,[9] showing that the onset of the high density inductive mode (ion current density ≥ 1 mA/cm^2) occurs at an ICP power above ~200 W in our system. While the ion current density was shown to continuously increase from 0.06 to 3.7 mA/cm^2 with the ICP power in the 50–1100 W range,[9] Fig. 5 shows that the InP etch rate tends to saturate to a typical value of 800 nm/min at high ICP powers, and even to show a decrease after a maximum value of ~900 nm/min achieved around 400 W ICP power. The main interesting result obtained at high ICP power concerns the etching profile, as illustrated in Figs. 6(a)–6(d). While an undercut profile resembling that reported in Ref. 3 is observed at moderate ICP powers (200–700 W), a transition to an almost vertical profile occurs when the ICP power is further increased. In Fig. 6(d), corresponding to 1000 W ICP power, a deposited layer is clearly present on the ridge sidewall. The same profile evolution with ICP power was observed in the 0.3–1 mT pressure range. An InP sample was thus etched using the HBr chemistry with the maximum ICP power of 1100 W for EDX-TEM inspection. The dc bias and pressure were fixed to −140 V and 0.5 mT, respectively, for comparison with the Cl_2-H_2 anisotropic process. The HBr flow rate was set to 10 SCCM, close to the maximum achievable flow-rate value at 0.5 mT pressure. A highly anisotropic etching was achieved under these conditions, since the 0.2-μm diameter pillars were safely etched to an etch depth of 3 μm, as shown in Fig. 7(a) (aspect ratio > 15).

The TEM image of a HBr pillar is shown in Fig. 7(b) and the results of the EDX analysis are reported in Table I. TEM inspection evidenced that an amorphous layer is present on the pillar sidewalls. As for all Cl_2-based previous experiments, the layer is thicker on the top (70 nm thickness) than on the bottom of the pillars (3 nm thickness). For the same etch depth, it is thicker than in the case of the Cl_2-H_2 chemistry. The pillar sidewalls are very smooth, comparable to the case of the Cl_2-H_2 chemistry. The composition (atomic percentage) of the amorphous layer presents some similarities with the Cl_2-H_2 process: the layer appears to be Si rich, the Si/O ratio approaching 3/1 for HBr. Slight differences also

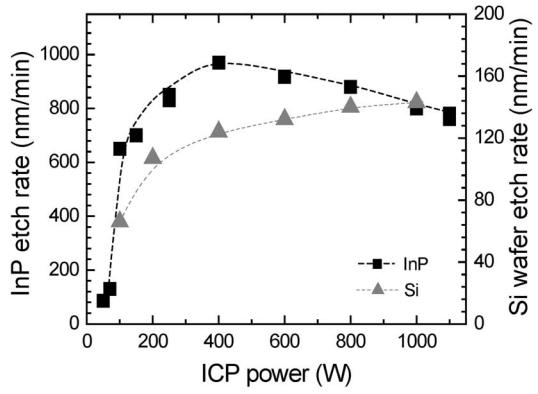

FIG. 5. InP etch rate (squares, left vertical axis) and Si wafer etch rate (triangles, right vertical axis) measured as a function of ICP power. The other etching parameters are −140 V dc bias, 1 mT, and 10 SCCM HBr flow rate. The electrode temperature was fixed to 150 °C, InP samples nonthermalized. The dashed lines are guides to the eyes.

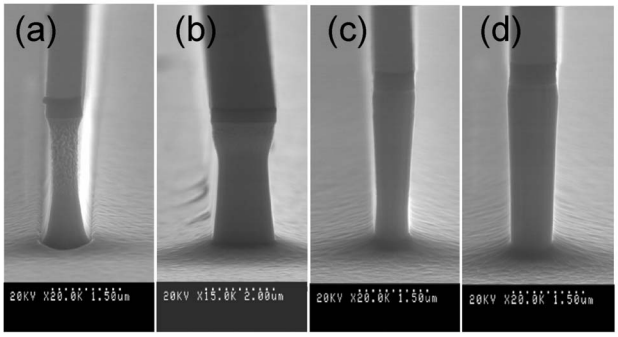

FIG. 6. SEM image of the ridge profiles etched with ICP powers of (a) 200 W, (b) 500 W, (c) 800 W, and (d) 1000 W. The other etching conditions are those of Fig. 5.

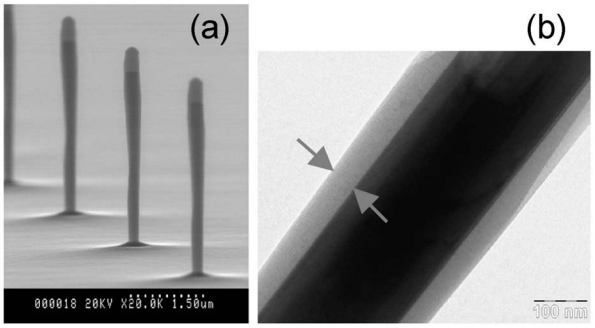

FIG. 7. (a) SEM image of 0.2-μm diameter pillars etched with 10 SCCM HBr flow rate, 1100 W ICP power, −140 V dc bias, and 0.5 mT. The electrode temperature was fixed to 130 °C, InP samples nonthermalized. (b) Typical TEM image of the top part of a pillar.

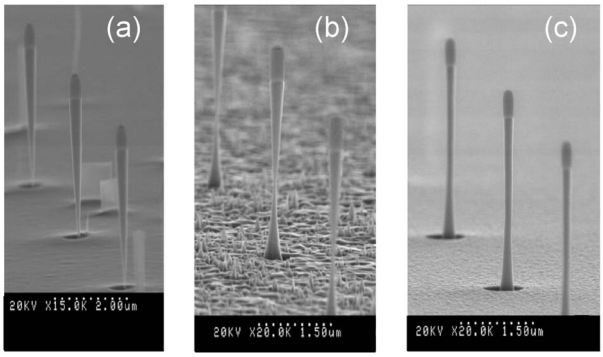

FIG. 8. SEM images of the pillars of smallest diameter etched to an etch depth of 3 μm with $Cl_2-H_2-O_2$ [(a) 0.3 μm diameter], Cl_2-O_2 [(b) 0.3 μm diameter], and $HBr-O_2$ [(c) 0.2 μm diameter].

appear when comparing the data of Table I. First, a small amount of Br is still incorporated in the layer, while only traces of Cl ($<\sim 2\%$) have been identified by EDX analysis. However, it should be noted that because of the *ex situ* procedure, the possible oxydization of the passivation layer due to reaction with ambient air and the possible desorption of Cl and Br constituents is not well controlled. Second, a moderate amount of P element (7%–9%) is incorporated in the layer. The P signal could not come from the inner InP part of the pillar, since the amorphous layer thickness (70 nm) is significantly larger than the spatial resolution of the EDX analysis. From our observations, we first conclude that anisotropic InP ICP etching is possible in HBr chemistry as for the Cl_2-H_2 chemistry. In both cases, anisotropy is achieved due to the deposition of a Si-rich passivation layer, the silicon coming from the etching of the 4 in. Si wafer used as the sample tray. Our results also suggest that the introduction of HBr can enhance the formation of the Si layer; for the same etch depth, a thicker layer is indeed obtained with HBr than with Cl_2-H_2, and a higher aspect ratio is achieved with HBr. It is worthwhile to compare this result with those reported in the domain of microelectronics and Si gate etching with $HBr-Cl_2-O_2$ inductively coupled plasmas. In-depth investigation has been carried out in the past decade to explain the anisotropy of this process, and it was demonstrated that the etching of sub-100-nm Si gate was possible due to the deposition of a SiOCl or SiOBr passivation layer on the gate sidewall.[14,15] Moreover, it was reported that the use of HBr in the gas mixture significantly improves the process,[16] the exact physicochemical origin of this effect being not yet well explained to our knowledge.

V. O_2 ADDITION

Since *ex situ* analysis evidenced that the amorphous layer present on the sidewall was mainly composed of amorphous SiO_x, we intentionally added oxygen to the Cl_2-based and HBr processes. The formation of a more stoichiometric and denser SiO_2 layer might indeed be favored *in situ* by adding oxygen, leading to higher achievable aspect ratio.

A rough process optimization was preliminary conducted for this purpose, starting from the Cl_2 process, the anisotropic Cl_2-H_2 process ($Cl_2/H_2=18/10$ SCCM), and the HBr process used for EDX-TEM analysis. In all cases, the dc bias and pressure were fixed to −140 V and 0.5 mT, respectively. For the Cl_2 and Cl_2-H_2 chemistries, the ICP power and the total gas flow rate were fixed to 800 W and 28 SCCM, respectively. For the HBr chemistry, the total flow rate was of 10 SCCM, and the ICP power was of 1100 W. The main general tendencies observed in the three cases were similar. On one hand, the addition of a small amount of oxygen slightly improves the process anisotropy. On the other hand, increasing the O_2 percentage in the gas mixture led to the apparition of a grassy surface probably due to micromasking effects. In order to investigate the change in the thickness and/or composition of the amorphous layer by EDX-TEM, the O_2 flow rate was consequently fixed to the maximum achievable value before the development of grass on the etched surface. This condition corresponded to 2, 1, and 1 SCCM for the Cl_2, Cl_2-H_2, and HBr processes, respectively. SEM images of the pillars of smallest diameter safely etched to an etch depth of 3 μm are reported in Figs. 8(a)–8(c) for the three cases. It can be deduced from the figure that adding O_2 to the pure Cl_2 process, while maintaining a nongrassy etched surface, is not sufficient to significantly improve the etching anisotropy. In the Cl_2-H_2 and HBr cases, the verticality of the pillar sidewall is slightly improved, if one compares Figs. 4(d) to 8(a), and Figs. 7(a) to 8(c). The highest aspect ratio is obtained with the $HBr-O_2$ chemistry. Indeed, 0.2-μm diameter pillars could be etched to an etch depth of 3.5 μm, corresponding to an aspect ratio larger than 17. Typical TEM images of the etched pillars are reported in Figs. 9(a)–9(c), and the composition and average thickness of the amorphous layer are reported in Table II.

When comparing the results of Tables I and II for the Cl_2-H_2 and the $Cl_2-H_2-O_2$ processes, it is obvious that O_2 addition led to a change in the deposition layer: it is slightly thicker (15–20 nm on the top part of the pillar), and, more important, its *ex situ* composition is modified from Si rich with Si/O ratio ~ 1, to that of a more stoichiometric SiO_2-like layer. A similar evolution in the passivation layer composition can be observed when comparing Tables I and II for the HBr chemistry. The intentional addition of 1 SSCM

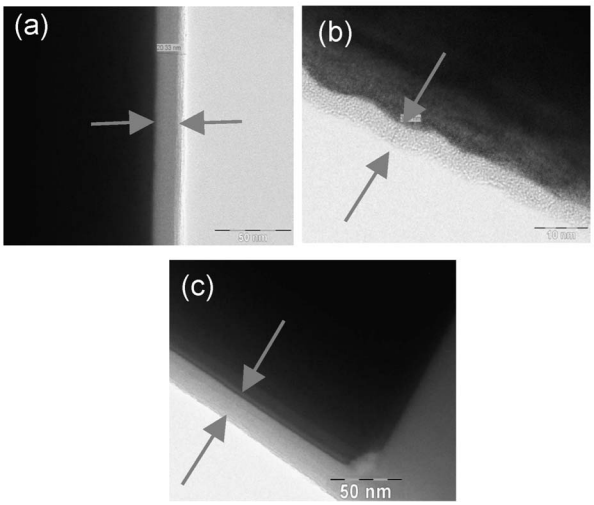

FIG. 9. TEM images of the top part of pillars etched with (a) $Cl_2-H_2-O_2$, (b) Cl_2-O_2, and (c) $HBr-O_2$.

of O_2 in the process modified the passivation layer into SiO_2. For both the $Cl_2-H_2-O_2$ and the $HBr-O_2$ processes, TEM inspection reveals that the sidewalls of the etched pillars are extremely smooth. On the other hand, TEM inspection confirmed that adding up to 2 SCCM of O_2 to Cl_2 only, is not sufficient to ensure anisotropic etching. The amorphous layer consists of silicon oxide, and its thickness is slightly increased (3–5 nm on the top part of the pillar, 2–3 nm on the bottom part) compared to the Cl_2 process, but it is clearly not thick enough to ensure straight and smooth InP sidewalls.

EDX-TEM analysis has evidenced that, in any case, a significant amount of oxygen is systematically incorporated in the passivation layer. The presence of oxygen can come from a reaction of the layer with ambient air, since our analysis is performed *ex situ*. It was indeed reported from x-ray photoelectron spectroscopy (XPS) analysis of the sidewalls of poly-Si patterns etched with $Cl_2-HBr-O_2$ gas mixtures that Cl or Br desorption and substitution by oxygen take place under air exposure.[16] However, it should be considered that oxygen in the plasma can also come from the sputtering of the inner parts of the reactor, especially in our very low pressure conditions since decreasing the pressure leads to an increase of the plasma potential as observed from separate Langmuir probe measurements.[17] Moreover, as seen from the results obtained when O_2 is added *in situ* to the gas mixture, only a very small proportion of oxygen is sufficient to increase the O atomic concentration in the redeposition layer. We believe that, in a similar way as for the formation of the SiOCl passivation layer during ICP etching of silicon with $Cl_2-HBr-O_2$ chemistry, a minimum amount of oxygen is needed in the plasma to allow for the passivation layer to build up on the InP sidewalls. In the detailed XPS analysis carried out in Ref. 16, it was suggested that the SiOCl or SiOBr passivation layer deposited on the Si sidewalls is densified and transformed in a more SiO_2-like layer in the presence of oxygen. The possible densification of the layer in the presence of oxygen could also take place in our case and could explain the better anisotropy and the extremely low sidewall roughness obtained with the $Cl_2-H_2-O_2$ and the $HBr-O_2$ processes.

VI. Cl_2–N_2 CHEMISTRY

Cl_2-N_2 chemistry has also been developed for the anisotropic etching of ridge waveguides[18] or of low-threshold laser ring resonators,[6] and it may represent an alternative to the Cl_2-H_2 chemistry. As for Cl_2-H_2, the physicochemical mechanism involved in the anisotropic etching has not been investigated yet, therefore, we etched InP samples with Cl_2-N_2 for comparison. In order to obtain conditions leading to etch rate, surface and sidewall smoothness compatible with our analysis procedure, we preliminary conducted a rough process optimization. The final process parameters are not far from those proposed in earlier reports,[4,6,18] and are the result of the following experimental observations.

For comparison purpose, we started from parameters close to those of the Cl_2-H_2 process, i.e., 800 W ICP power (approximately same positive ion density), −140 V dc bias (approximately same positive ion energy neglecting mass difference and small changes in plasma potential), 0.5 mT pressure (same total concentration of plasma species). The total flow rate was fixed to 20 SCCM corresponding to the highest achievable N_2 flow rate at 0.5 mT with our pumping system. A 4 in. Si wafer was used as the sample tray.

The InP etch rate measured as a function of N_2 percentage in the Cl_2-N_2 mixture is reported in Fig. 10. Addition of a very small amount of N_2 (10% or less) led to the apparition of an extremely rough and grassy surface, preventing any rigorous measurement of the etch rate. At least 30% of N_2 should be added to recover a not too grassy surface. The

TABLE II. InP etch rate, 4 in. Si wafer etch rate (and Si equivalent flux, Φ_{Si}), average thickness of the passivation layer measured on the top part of the pillar, and average passivation layer composition in atomic percentage, for the Cl_2-O_2, $HBr-O_2$, and $Cl_2-H_2-O_2$ process. In the Cl_2-O_2 case, the thickness of the passivation layer is smaller than the spatial resolution of the EDX analysis.

Process	Etch rate (nm/min)		Passivation layer							
				Average composition (at %)						
Gas flow rate (SCCM)	InP	Si [Φ_{Si} (SCCM)]	Thickness (nm)	Si	O	Br	Cl	P	In	Al
$Cl_2(28)/O_2(2)$	3000	250 (3.2)	3–5	43	57	···	···	···	···	···
$HBr(10)/O_2(1)$	690	130 (1.7)	20	35	60	2	···	3	···	···
$Cl_2(18)/H_2(10)/O_2(1)$	910	160 (2.1)	20	33	65	···	···	···	···	2

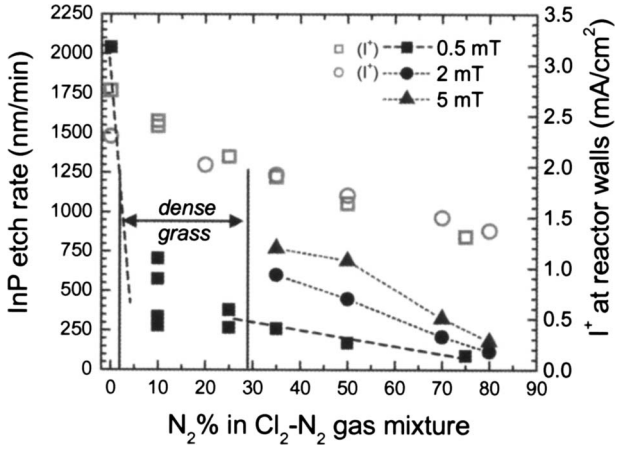

FIG. 10. Left axis: InP etch rate measured as a function of N_2% in the Cl_2-N_2 mixture at a pressure of 0.5 mT (black squares), 2 mT (black circles), and 5 mT (black triangles). Right axis: Positive ion current density measured as a function of N_2% at a pressure of 0.5 mT (open squares) and 2 mT (open circles). The other etching parameters are 800 W ICP power, −140 V dc bias, 20 SCCM total flow rate, $T_{electrode}$=150 °C, InP samples nonthermalized.

intermediate unstable region at low to moderate N_2 percentage has been almost systematically observed and has generally been related to a strongly unbalanced etching of P and In elements due to the opposite effects of Cl etching and surface nitridation, having a different equilibrium for In and P.[4,7] Simultaneously, the etch rate is significantly reduced. Maintaining the pressure and dc bias values to 0.5 mT and −140 V, respectively, led to such a low InP etch rate, that 3 μm high pillars could not been obtained due to selectivity issues. The pressure was consequently increased to a value of 2 mT compatible with the etching of 3 μm high pillars, while keeping the same dc bias. As can be observed from Fig. 10, the etch rate is indeed increased by increasing the pressure. Similar optimized process parameters have been proposed in Refs. 4, 6, and 18.

The positive ion current density measured at the reactor walls at 0.5 and 2 mT pressure conditions is also reported in Fig. 10. For an ICP power of 800 W, the ion current density is roughly of the same order of magnitude as that measured for the Cl_2-H_2 chemistry[2] (i.e., in the 1–2 mA/cm^2 range, with a decrease in ion current density when N_2 percentage or pressure is increased).

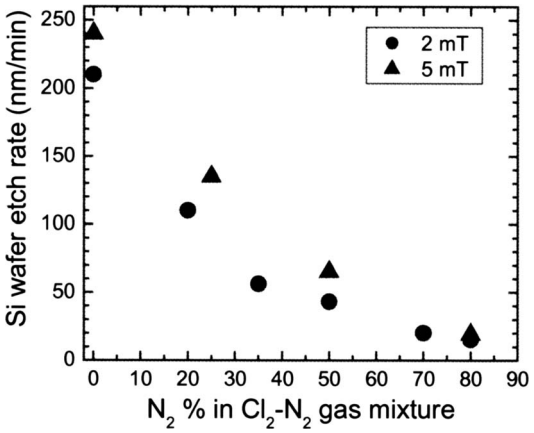

FIG. 11. 4 in. Si wafer etch rate measured as a function of N_2% in the Cl_2-N_2 mixture at a pressure of 2 mT (black circles) and 5 mT (black triangles). The other etching parameters are those of Fig. 10.

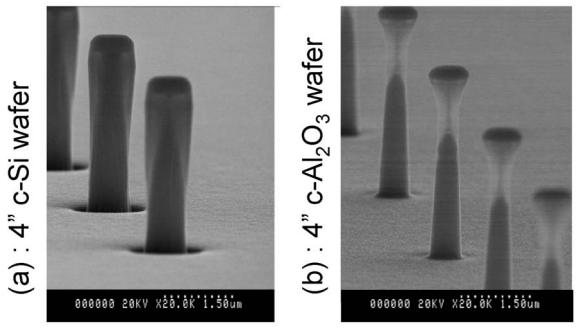

FIG. 12. SEM images of the 0.7-μm diameter pillars etched with 800 W ICP power, −140 V dc bias, 2 mT, 70% N_2, 20 SCCM total flow rate, using a c-Si wafer (a) and a c-Al_2O_3 wafer (b) as the sample tray. $T_{electrode}$ =150 °C, InP samples nonthermalized.

The 4 in. Si wafer etch rate is reported as a function of N_2 percentage in Fig. 11. The Si etch rate decreases when the N_2 % is increased, and becomes very low (<20 nm/min) at high N_2 %. However, it cannot be neglected compared to the InP etch rate, which is also strongly reduced at high N_2 %. Before TEM-EDX analysis, the possible influence of the Si reaction products on the process anisotropy was checked by successively etching two InP samples with a c-Si tray and a c-Al_2O_3 tray, while keeping all other parameters unchanged (e.g., 800 W ICP power, −140 V dc bias, 2 mT, 20 SSCM total flow rate, 70% N_2). SEM images of the 0.7-μm diameter etched pillars are reported in Figs. 12(a) and 12(b). The influence of the Si coverplate on the pillar profile is clearly observed.

The SEM images of 0.6-μm diameter pillars etched to an etch depth of 3 μm are reported in Figs. 13(a)–13(c) for 35% of N_2 and 2 mT pressure (case A), for 50% N_2 and 2 mT pressure (case B), and for a limit case corresponding to 70% N_2 and 5 mT pressure (case C). Typical TEM images of the etched pillars are reported in Figs. 14(a)–14(c), and the *ex*

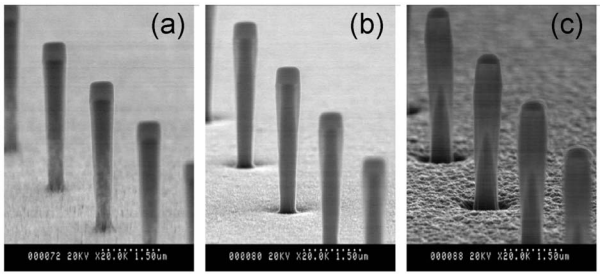

FIG. 13. SEM images of the 0.6-μm diameter pillars etched to an etch depth of ~3 μm with (a) 2 mT and 35% N_2, (b) 2 mT and 50% N_2, and (c) 5 mT and 70% N_2. The other etching parameters are 800 W ICP power, −140 V dc bias, 20 SCCM total flow rate. $T_{electrode}$=150 °C, InP samples nonthermalized.

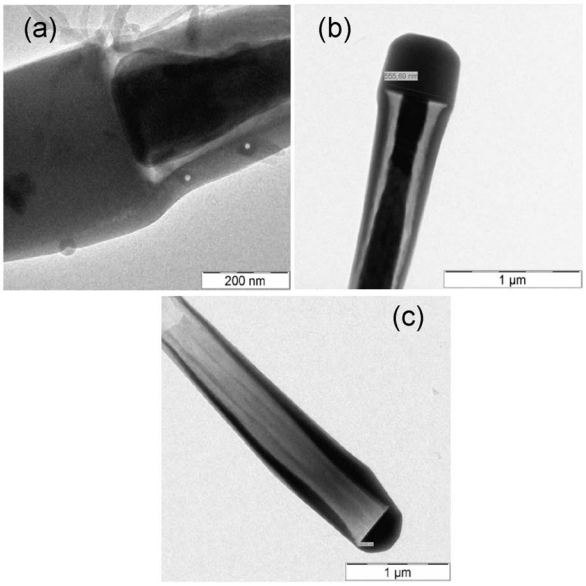

FIG. 14. TEM images of the top part of pillars etched with (a) 35% N_2 at 2 mT, (b) 50% N_2 at 2 mT, and (c) 70% N_2 at 5 mT. The two small white holes in (a) have been drilled in the redeposition layer by the electron beam spot used for EDX analysis.

situ analysis of the amorphous layer composition can be found in Table III.

It was deduced from TEM inspection that the amorphous layer formed on the pillar sidewalls was very thick: more than 100 nm on the top part of the pillars in cases A, B, and C. This layer also significantly extends under the SiN_x mask, which constitutes a strong difference with the Cl_2-H_2 or HBr chemistry. Figures 14(a) and 14(b) show that an intermediate region exists between the redeposition layer and the pillar core. While it was deduced from EDX analysis that the core was InP, the intermediate region is of very low density and almost empty. In the limit case C, all the InP crystalline material has disappeared from the pillar core on the top part of the pillar, which is only composed of the intermediate region and of the redeposition layer. Finally, the redeposition layer is very porous: the electron beam is able to destroy the layer, as evidenced on Fig. 14(a) where the small holes are formed by the electron beam impact during EDX analysis. A very interesting result on the Cl_2-N_2 chemistry is about the layer composition. First, it contains almost no N element, which indicates that nonvolatile InN or PN complex that could prevent Cl lateral etching are not readily formed on the sidewalls. The exact N composition is difficult to estimate, because the *K* line of N element is screened by both O and C *K* lines (the C signal coming mainly from the carbon membrane) leading to a somewhat noisy deconvolution of each peak. However, the N atomic percentage is definitely lower than 4% in any case. Second, the amorphous layer is mainly composed of Si and O, with a Si/O ratio around 1/2 to 1/3. Third, a significant amount of P is incorporated in the amorphous layer (from 12% to 25%), while In is only detected as weak traces ($<0.5\%$). We conclude from our results that the origin of the apparent anisotropy observed during InP ICP etching with Cl_2-N_2 is related to the formation of a thick SiOP amorphous layer. However, under our etching conditions, the layer is very porous, and does not prevent a lateral underetching of the InP material. We suggest two possible origins for the formation of this phosphorous-rich layer. XPS analysis of InP surfaces ICP etched with chlorine at a sufficiently high temperature have already evidenced that the surface is generally P rich,[19] and not In rich as could be expected due to the lower volatility of the $InCl_x$ products compared to the PCl_x products. Adding N_2 to Cl_2 may contribute to further suppress P removal compared to In removal. This assumption implies that N element either strongly suppresses the PCl_x desorption, or inhibits the formation of the PCl_x complex. Another possible mechanism could be due to the formation of stable Si(O)P bonds during the deposition of the Si-rich passivation layer, while bonding with In is not favored. The correct explanation for the formation of the SiOP layer on InP sidewalls during Cl_2-N_2 etching needs further investigation and is beyond our first preliminary investigation.

VII. CONCLUSION

We have used EDX-TEM *ex situ* analysis to demonstrate that the good anisotropy observed during ICP etching of InP using Cl_2 as the main etching gas is due to the formation of a Si-rich passivation layer on the InP sidewalls, when a Si wafer is used as the sample tray. Moreover, we have evidenced that the layer redeposition is enhanced by H addition in the plasma, leading to anisotropic etching suitable for the definition of photonic elements. We have demonstrated that similar results can be obtained in HBr chemistry when the ICP power is increased. A thicker and even more Si-rich passivation layer is obtained in this case. The EDX-TEM analysis has also evidenced that a significant amount of oxy-

TABLE III. InP etch rate, 4 in. Si wafer etch rate (and Si equivalent flux, Φ_{Si}), average thickness of the passivation layer measured on the top part of the pillar, and average passivation layer composition in atomic percentage, for the Cl_2-N_2 chemistry in cases A, B, and C.

Process	Etch rate (nm/min)		Passivation layer							
				Average composition (at %)						
Gas flow rate (SCCM)	InP	Si [Φ_{Si} (SCCM)]	Thickness (nm)	Si	O	N	Cl	P	In	Al
$Cl_2(13)/N_2(7)-(A)$	600	56 (0.72)	>100	22	57	3	1.7	15	0.3	1
$Cl_2(10)/N_2(10)-(B)$	360	40 (0.78)	>100	21	52	4	4	17	···	2
$Cl_2(6)/N_2(14)-(C)$	180	19 (0.25)	>100	20	48	4	3	22	···	3

gen is systematically incorporated in the passivation layer. This could partly result from the desorption of Cl or Br atoms and substitution by oxygen under air exposure. However, we believe that oxygen coming from the inner parts of the reactor is present in the plasma and contributes to the buildup of the passivation layer. *In situ* or quasi-*in-situ* techniques have to be developed to confirm the exact amount of O and of Cl (or Br) incorporated in the passivation layer when it builds up. The *ex situ* analysis remains anyway of practical interest for further postprocessing steps such as chemical treatment, regrowth, etc.

We suggest that the passivation mechanism evidenced during InP etching using a Si wafer as the sample tray resembles that already identified in $Cl_2-HBr-O_2$ ICP Si gate etching in microelectronics. A passivation layer consisting of SiOCl or SiOBr is deposited on the gate sidewall, and HBr addition leads to a more anisotropic etching of the gate.

The Cl_2-N_2 chemistry has been compared to the Cl_2-H_2 and HBr chemistries, for similar ICP power and same dc bias. We have observed a thick SiOP amorphous layer on the InP sidewalls. We have evidenced that in our etching conditions, this layer is porous and cannot actually prevent the lateral etching of the InP material. No N element has been found in the amorphous layer indicating that InN or PN complexes are not present, in contrast to other analysis performed on planar etched surface. Moreover, In is clearly removed from the InP material and can diffuse through the layer, whereas P is blocked or reincorporated in this layer. We suggest that the Cl_2-H_2 or the HBr chemistry may be more suitable than the Cl_2-N_2 chemistry for the definition of ridge waveguides, deeply etched facets, ring resonators, or micropillar cavities; first, because the semiconductor material is preserved beneath the thin passivation layer, and second, because the removal of the amorphous layer and the restoration of the InP surface by chemical treatment after dry etching might be performed more easily in the Cl_2-H_2 case (removal of a SiO_x layer) than in the Cl_2-N_2 case (phosphorous-rich amorphous layer).

Finally, for future industrial conditions where the diameter of the InP wafer to be etched may be larger than 2 in. and may completely cover or even replace the Si tray, it can be predicted that the anisotropic etching will not be maintained if the gas mixture is not changed. From our results, we suggest that the addition of a Si-containing gas such as $SiCl_4$ (or SiH_4) to the $Cl_2-H_2-O_2$ or $HBr-O_2$ mixture could allow for maintaining anistropic etching with a similar sidewall passivation mechanism.

ACKNOWLEDGMENTS

The authors thank Dr. Luc Le Gratiet from Laboratoire de Photonique et de Nanostructures for his precious assistance in e-beam lithography. Ko-Hsin Lee of LPN is acknowledged for fruitful discussions on Cl_2-N_2 ICP etching of InP-based nanostructures.

[1] S. L. Rommel *et al.*, J. Vac. Sci. Technol. B **20**, 1327 (2002).
[2] S. Guilet, S. Bouchoule, C. Jany, C. S. Corr, and P. Chabert, J. Vac. Sci. Technol. B **24**, 2381 (2006).
[3] Y. S. Lee, M. DeVre, D. Lishan, and R. Weestreman, G. Kim, 15th International Conference on Indium Phosphide and Related Materials, Santa Barbara, CA, 12–16 May 2003 (unpublished), Paper No. TuA2.6 (Postdeadline), p. 78.
[4] S. Myakuni, R. Hattori, K. Sato, H. Takano, and O. Ishihara, J. Appl. Phys. **78**, 5734 (1995).
[5] Y. Suzuki, H. Kumano, W. Tomota, N. Sanada, and Y. Fukuda, Appl. Surf. Sci. **162–163**, 172 (2000).
[6] S. Park, S.-S. Kim, L. Wang, and S.-T. Ho, IEEE J. Quantum Electron. **41**, 351 (2005).
[7] P. Strasser, R. Wuest, F. Robin, D. Erni, and H. Jackel, J. Vac. Sci. Technol. B **25**, 387 (2007).
[8] B. Docter, E. J. Geluk, M. J. H. Sander-Jochem, F. Karouta, and M. K. Smit, 19th International Conference on Indium Phosphide and Related Materials, Matsue, Japan, 14–18 May 2007 (unpublished), p. 226.
[9] S. Bouchoule, S. Azouigui, G. Patriarche, S. Guilet, L. Le Gratiet, A. Martinez, F. Lelarge, and A. Ramdane, 19th International Conference on Indium Phosphide and Related Materials, Matsue, Japan, 14–18 May 2007 (unpublished), p. 218.
[10] L. Gatilova, S. Bouchoule, S. Guilet, and P. Chabert, AVS 54th International Symposium, Seattle, WA, 14–19 October 2007 (unpublished), Paper No. PS-MoA3.
[11] A. Matsutani, H. Ohtsuki, F. Koyama, and K. Iga, Jpn. J. Appl. Phys., Part 1 **41**, 3147 (2002).
[12] E. Zhirnov, S. Stepanov, W. N. Wang, Y. G. Shreter, D. V. Takhin, and N. I. Bochkareva, J. Vac. Sci. Technol. A **22**, 387 (2004).
[13] L. Deng, A. L. Goodyear, and M. Dineen, Proc. SPIE **5280**, 838 (2004).
[14] F. H. Bell and O. Joubert, J. Vac. Sci. Technol. B **14**, 1493 (1996).
[15] C. C. Cheng, K. V. Guinn, I. P. Herman, and V. M. Donnelly, J. Vac. Sci. Technol. A **13**, 214 (1995).
[16] L. Desvoivres, L. Vallier, and O. Joubert, J. Vac. Sci. Technol. B **19**, 420 (2001).
[17] C. S. Corr, S. Guilet, S. Bouchoule, and P. Chabert (unpublished).
[18] J. Lin, A. Leven, N. G. Weimann, Y. Yang, R. F. Kopf, R. Reyes, and Y. K. Chen, J. Vac. Sci. Technol. B **22**, 510 (2004).
[19] B. Liu *et al.*, Mater. Sci. Semicond. Process. **9**, 225 (2006).